J Nanopart Res (2013) 15:1522
DOI 10.1007/s11051-013-1522-8

BRIEF COMMUNICATION

A copper cluster protected with phenylethanethiol

Anindya Ganguly · Indranath Chakraborty · Thumu Udayabhaskararao · Thalappil Pradeep

Received: 10 December 2012 / Accepted: 15 February 2013

Abstract A copper cluster protected with 2-phenylethanethiol (PET) exhibiting distinct optical features in UV/Vis spectroscopy is reported. Matrix-assisted laser desorption ionisation mass spectrometry of the cluster shows a well-defined molecular ion peak at *m*/*z* 5,800, assigned to $\sim Cu_{38}(PET)_{25}$. Fragmented ions from the cluster show the expected isotope patterns in electrospray ionisation mass spectrometry. The as-synthesized cluster was well-characterised using other tools as well. Clusters undergo decomposition in about 2 h after synthesis as a metallic few-atom core of copper is highly unstable. The products of decomposition were also characterised.

Keywords Atomically precise · Cu cluster · 2-Phenylethanethiol · MALDI MS · ESI MS

Introduction

Noble metal quantum clusters (Lu and Chen 2012; Yuan et al. 2011) belong to an area of intense activity in the recent past. They are remarkable because of their unique absorption (Chaki et al. 2008; Zhu et al. 2008; Habeeb and Pradeep 2011; Mathew et al. 2011) and emission (Xavier et al. 2012; Rao and Pradeep 2010) features as well as due to novel applications (Retnakumari et al. 2010; Muhammed et al. 2009; Goswami et al. 2011; Mathew et al. 2012; Haruta 2005; Xie et al. 2012). Au_{25} (Chaki et al. 2008; Zhu et al. 2008; Shichibu et al. 2005; Shibu et al. 2008), Au_{38} (Pei et al. 2008) and Au_{102} (Jadzinsky et al. 2007) clusters have been investigated in detail due to their enhanced stability. Several silver clusters, e.g., Ag_7 (Rao and Pradeep 2010; Udayabhaskararao et al. 2012), Ag_8 (Rao and Pradeep 2010), Ag_9 (Rao et al. 2010), Ag_{32} (Guo et al. 2012), Ag_{75} (Chakraborty et al. 2012b) and Ag_{152} (Chakraborty et al. 2012a), have also been reported recently. However, efforts on the preparation of monolayer-protected Cu clusters are limited (Vilar-Vidal et al. 2010; Salorinne et al. 2012; Jia et al. 2012; Saumya and Rao 2012; Wei et al. 2011) while there are several reports on copper nanoparticles (Bakshi et al. 2007; Nishida et al. 2011; Prucek et al. 2009; Wei et al. 2010). In terms of applications, copper is more appealing for its availability, lower cost, catalytic activity and electrical conductivity. In this communication, we report a facile one-pot synthesis of a new 2-phenylethanethiol (PET)-protected copper cluster. It has been characterised using UV/Vis absorption spectroscopy, mass spectrometry, high-resolution transmission electron microscopy (HRTEM), X-ray photoelectron spectroscopy and photoluminescence spectroscopy.

Electronic supplementary material The online version of this article (doi:10.1007/s11051-013-1522-8) contains supplementary material, which is available to authorized users.

A. Ganguly · I. Chakraborty · T. Udayabhaskararao · T. Pradeep (✉)
DST Unit of Nanoscience (DST UNS), Department of Chemistry, Indian Institute of Technology Madras, Chennai 600 036, India
e-mail: pradeep@iitm.ac.in

Published online: 12 March 2013

Experimental section

Materials

All the chemicals were commercially available and used without further purification. The used chemicals and solvents are: copper sulphate pentahydrate ($CuSO_4 \cdot 5H_2O$), cupric acetate, cupric chloride, 2-phenylethanethiol, sodium borohydride ($NaBH_4$), ethanol, acetonitrile, tetrahydrofuran (THF) and toluene.

Synthesis of $\sim Cu_{38}(PET)_{25}$

A solid-state route (Rao et al. 2010) was followed for the synthesis of copper clusters protected with PET. Initially, 47 mg of copper sulphate pentahydrate and 150 μL of PET were taken in an agate mortar and ground well for 10 min, then 80 mg of $NaBH_4$ was added and further ground for two more minutes followed by extraction of clusters in ethanol. All the operations were done in laboratory atmosphere (30–35 °C, 80 % relative humidity). The crucial aspect of this procedure is the limited supply of water needed for the reduction, which becomes available from the laboratory atmosphere as well as from the ethanol used for subsequent washing. A solution of the as-synthesized clusters in ethanol was light pink in colour (Fig. 1b). Sequential photographs of the synthesis are given in Supplementary Fig. S1. Blue colour of the copper salt changed to yellow after grinding with PET because of the formation of Cu–thiolates. Reduction of copper thiolate with $NaBH_4$ led to a black paste, which changed to pink when extracted in ethanol.

Characterisation of $\sim Cu_{38}(PET)_{25}$

Perkin Elmer Lambda 25 instrument was used for measuring UV/Vis spectra in the range of 200–1,100 nm. X-ray photoelectron spectroscopy (XPS) measurements were carried out using an Omicron ESCA Probe spectrometer with polychromatic MgKα X-rays ($h\upsilon = 1{,}253.6$ eV). The samples were spotted as drop-cast films on a sample stub. Constant analyzer energy of 20 eV was used for the measurements. The samples were prepared as fast as possible and were inserted into high vacuum within 5 min of synthesis to avoid aerial oxidation. Luminescence measurements were measured with a Jobin Vyon NanoLog instrument. The band passes for excitation and emission were set as

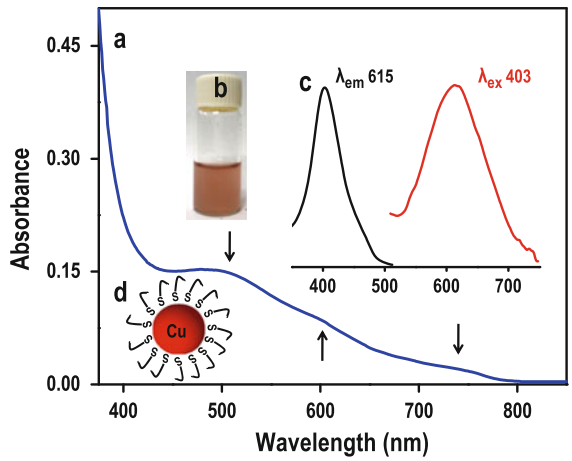

Fig. 1 UV/Vis absorption spectrum of the as-synthesized Cu@PET cluster (*a*) which shows three features at 500, 600 and 750 nm indicated by *arrows*. *Insets* (*b*) Photograph of the cluster solution showing *light pink colour*. (*c*) Luminescence excitation and emission spectra of Cu@PET cluster which emits at 615 nm upon excitation at 403 nm. (*d*) A cartoon representation of the cluster. (Color figure online)

2 nm. Matrix-assisted desorption ionisation mass spectrometry (MALDI MS) analysis were conducted using a Voyager-DE PRO Bio-spectrometry Workstation from Applied Bio-systems. A pulsed nitrogen laser of 337 nm was used for the MALDI MS analysis. Mass spectra were collected in negative ion mode and were averaged for 100 shots. Mass studies were conducted using an electrospray mass spectrometry (ESI MS) system, LTQ XL (Thermo scientific). Sample was taken in ethanol which was electrosprayed for analysis. High-resolution transmission electron microscopy of clusters was carried out with a JEOL 3010 instrument. The samples were drop casted on carbon-coated copper grids and allowed to dry in vacuum desiccators. Scanning electron microscopic (SEM) and energy-dispersive X-ray (EDAX) analyses were done in a FEI QUANTA-200 SEM. For measurements, samples were drop casted on an indium tin oxide-coated conducting glass and dried in vacuum. Powder XRD analysis of the decomposed sample was carried out using PANalytical X'pertPro diffractometer. X-ray diffractogram was collected in the 2θ range of 5–100°.

Results and discussion

The clusters show distinct step-like features at 500, 600 and 750 nm in the UV/Vis spectrum (Fig. 1a).

Interestingly, the clusters emit at room temperature. They show an excitation maximum at 403 nm and an emission maximum at 615 nm (Fig. 1c). From the view point of stability, clusters are short lived: after about 40 min of preparation, they show signs of decomposition which was monitored by optical absorption spectroscopy. The data showed (Supplementary Fig. S2) gradual merging of two humps (at 500 and 600 nm) into one. All the humps disappeared completely after 2 h, indicating the decomposition of the clusters.

Mass spectrometry is an ideal and most useful tool to find the composition of the clusters (Rao and Pradeep 2010; Dass 2009). Matrix-assisted laser desorption ionisation mass spectrometry (MALDI MS) and electrospray ionisation mass spectrometry (ESI MS) studies were conducted on the clusters. It is known that trans-2-[3-(4-tert-butylphenyl)-2-methyl-2-propenylidene]malononitrile (DCTB) gives well-defined mass spectrum for PET-protected clusters (Knoppe et al. 2010). We too used DCTB as the matrix. MALDI MS showed a single peak at *m/z* 5,800 at lowest laser intensity, assigned to $\sim Cu_{38}(PET)_{25}$ (Fig. 2a). No other peak was seen in the mass spectrum indicating the existence of only one type of cluster. The peak showed systematic shift to lower mass numbers upon increasing the laser intensity. This is characteristic of such clusters (Chakraborty et al. 2012b) which show fragmentation upon increasing laser intensity as the metal core–ligand interaction is weak.

ESI MS was performed in the negative ion mode for understanding the composition and the fragmentation pattern (Fig. 2b) of the as-synthesized clusters (Fig. 2c). As in several instances reported in the literature, we could not observe the molecular ion feature in ESI MS. However, we observed peaks corresponding to some of the fragmented ions (Rao and Pradeep 2010) in the case of silver clusters. The isotope patterns matched exactly with the calculated patterns. For instance, the peaks of $[Cu_4(PET)_5]^-$, having an intensity maximum at *m/z* 941 and $[Cu_5(PET)_6]^-$, having an intensity maximum at *m/z* 1,141 (Fig. 2a, b) matched with their calculated patterns. Other identified fragments are $[Cu_{34}(PET)_{23}]^{2-}$, $[Cu_{30}(PET)_{22}]^{2-}$, $[Cu_{29}(PET)_{21}]^{2-}$, $[Cu_{28}(PET)_{18}]^{2-}$ and $[Cu_{28}(PET)_{17}]^{2-}$ with corresponding *m/z* values of 2,655, 2,459, 2,359, 2,124 and 2,056, noted with arrows in Fig. 2c (from right to left). The presence of specific fragments support the existence of a PET-protected cluster in solution.

Because of its low standard reduction potential (0.34 V), copper is prone to aerial oxidation. Therefore, XPS was used to study the oxidation state of copper in the cluster. In view of the aerial oxidation of the cluster, the sample was immediately inserted into the vacuum chamber and analyzed as fast as possible.

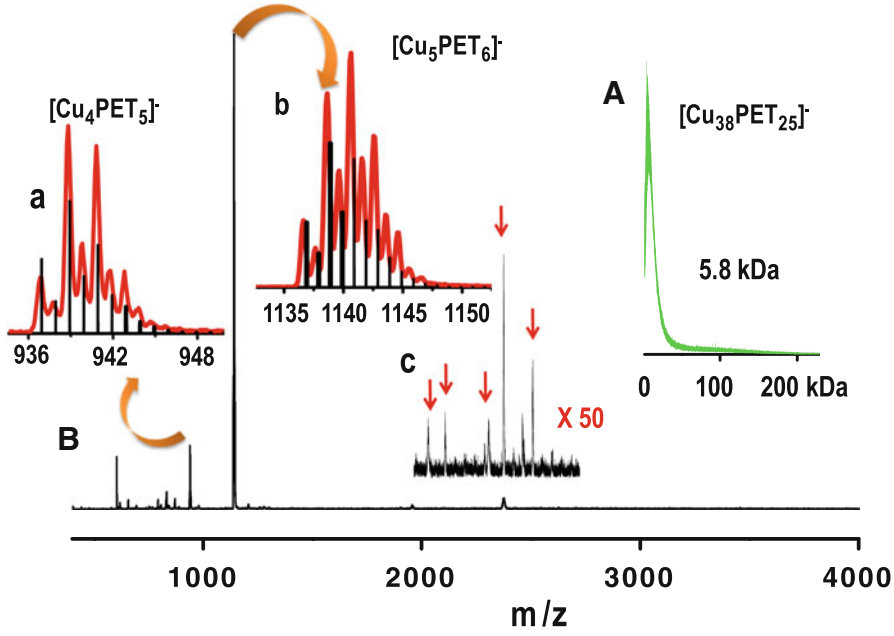

Fig. 2 (*A*) Linear negative ion MALDI mass spectrum of the Cu cluster. A molecular ion peak at *m/z* of 5,800 is clearly observed. The spectrum is shown from the minimum mass region measurable. (*B*) ESI MS data of Cu@PET cluster in the negative mode. *Insets* (*a*) and (*b*): Comparison of the observed isotope patterns (*red*) with the calculated patterns (*black*) of (*a*) $[Cu_4(PET)_5]^-$, *m/z* = 941, and (*b*) $[Cu_5(PET)_6]^-$, *m/z* = 1,141. (*c*) A *y*-axis expanded view of a selected region between *m/z* 2,000 and 3,000. Identified fragments are labelled with *red arrows*. (Color figure online)

No decomposition was seen within the time of sample transfer. The spectrum in the Cu 2*p* region shows two peaks: at 931.6 and 951.5 eV (Fig. 3), which have been assigned to $2p_{3/2}$ and $2p_{1/2}$ features of Cu (0). Binding energy (BE) of $2p_{3/2}$ in Cu^{+} of Cu_2O is 932.1 eV (Ai et al. 2009; Ghodselahi et al. 2008). So, Cu^{+} is unlikely to be present in the cluster. The most important observation is the absence of the satellite peaks. It is known that any species having d^9 (Cu^{2+}) configuration, such as CuO, would show satellite peaks which arise because of the configuration interaction of the $2p^5 3d^9 L$ (L = ligand, RS in the present case) final state (Ghijsen et al. 1988). Hence, the presence of Cu^{2+} is ruled out as well. The BE values are within the range of Cu(0) and Cu(I). Oxidation is very much facile in this size scale and this is likely to be the reason for the observed in-between values. This is the situation seen in Au and Ag clusters as well (Bootharaju and Pradeep 2011). XPS features of all other expected elements have been assigned in the survey spectrum and their expanded versions fitted exactly with that of the expected elements (Supplementary Fig. S3). The S 2*p* region shows a $2p_{3/2}$ feature at 162.9 eV, characteristic of thiolate. The C 1*s* binding energy seen is at 285.0 eV, characteristic of the ligand chain.

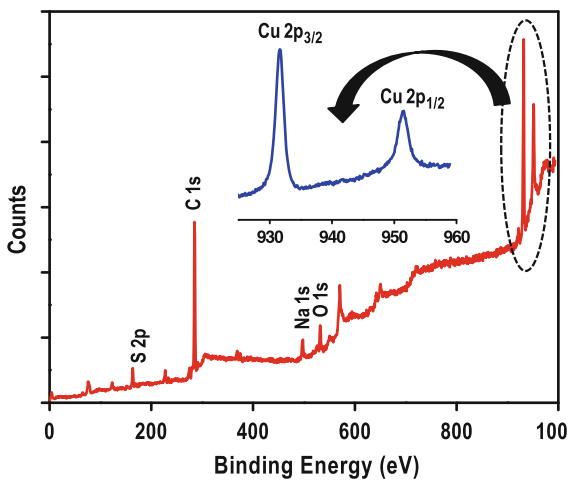

Fig. 3 XPS survey spectrum of Cu@PET cluster (*red*). It identifies the presence of copper, sulphur, carbon, sodium (a trace of Na, probably derived from $NaBH_4$) and oxygen. *Inset* Expanded XPS spectrum in the Cu 2*p* region of Cu@PET cluster (*blue*). Sharp peaks with narrow width are observed. The binding energy suggests the oxidation state of Cu to be close to zero and that of S 2*p* region is characteristic of thiolates. (Color figure online)

Various control experiments were carried out to optimize the conditions for synthesizing the cluster. First, molar ratio of PET with copper sulphate was varied (Supplementary Fig. S4). Five different molar ratios of copper sulphate to PET (1:1, 1:3, 1:5, 1:7 and 1:9) were tried. Among these, only the mixture with 1:5 ratio produced a light pink-coloured solution that showed distinct features in the optical absorption spectrum (Fig. 1a), while others did not have any characteristic features. Second, molar ratio of $NaBH_4$ was varied with respect to copper sulphate for the 1:5 sample. Five different molar ratios of copper sulphate and $NaBH_4$ (1:3, 1:7, 1:10, 1:13 and 1:15) were considered. Among these, the preparation with 1:10 ratio had distinct optical absorption features similar to that shown in Fig. 1a, while others had no characteristic optical absorption (Supplementary Fig. S5). Third, three different salts namely, cupric sulphate, cupric chloride and cupric acetate were used to find whether anion is playing any role for cluster formation/extraction. All of them produced samples of light pink colour; among which, the solution prepared from copper sulphate was most intense. In addition, sample from copper acetate showed the characteristic optical absorption features of $Cu_{38}(PET)_{25}$ which were significantly weaker than the same from cupric sulphate (Supplementary Fig. S6). Sample from cupric chloride did not show the desired optical absorption features. MALDI MS analyses were done for Cu@PET prepared from other two salts as well. The molecular ion peak at *m*/*z* 5,800 was observed for the sample prepared from cupric acetate indicating the presence of $\sim Cu_{38}(PET)_{25}$ in it (Supplementary Fig. S7). Fourth, different solvents (ethanol, acetonitrile, THF and toluene) were tried as extraction media. Among these, ethanol and acetonitrile were effective as solvents. The acetonitrile extract, however, showed weak absorption. Instead of showing three distinct features, it showed a single hump around 500 nm. On the other hand, THF and toluene were not able to extract the cluster as inferred by the absence of pink colour and characteristic absorption features (Supplementary Fig. S8).

Cluster formation was confirmed from the HRTEM images where the clusters appeared as tiny dots (Supplementary Fig. S9). The average diameter of the cluster is 1.4 nm, comparable to that of Au_{38} (Stellwagen et al. 2012). Upon longer electron beam irradiation, the dots grow gradually to form an aggregate, quite similar to that observed in the case of silver clusters

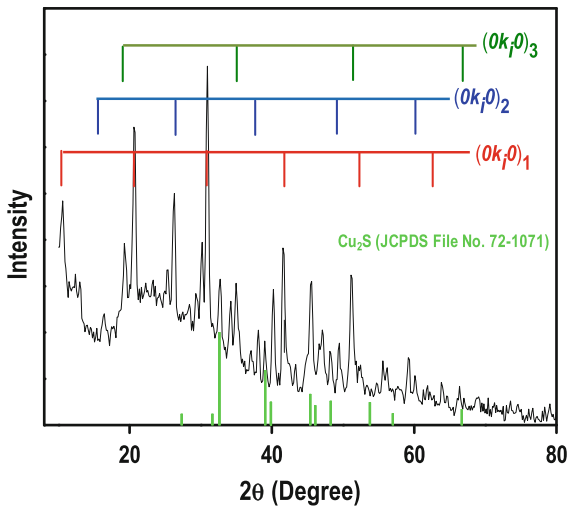

Fig. 4 Powder XRD pattern of the decomposed material consisting of a mixture of Cu_2S and copper thiolates. A few series of intense reflections, indexed as $(0k_i0)$, were observed because of polycrystalline copper thiolates. Successive diffraction peaks are because of differently structured [$(0k_i0)_1$, $(0k_i0)_2$ and $(0k_i0)_3$] multiple layers of copper thiolates. Three series are marked. The JCPDS pattern of Cu_2S is shown in *green*. (Color figure online)

(Rao and Pradeep 2010; Dhanalakshmi et al. 2012). From TEM/EDAX analysis, the Cu:S ratio was found to be 1:0.67, consistent with the proposed composition (1:0.65).

Scanning electron microscopy (SEM) is used to find out the presence of the expected elements in the cluster. It showed the desired elements (Supplementary Fig. S10). The Cu:S ratio was slightly different from the expected value, possibly due to excess thiol in that preparation. Excess thiol is found in the crystals of clusters.

The decomposed material (2 h after the synthesis) was converted to a powder by evaporating the solvent using a rotary evaporator and analyzed by powder X-ray diffraction (PXRD) which showed the presence of copper thiolates along with Cu_2S (Fig. 4) (JCPDS File No-72-1071). The PXRD pattern of longer chain thiolates consist of differently structured and stacked layers of Cu and S atoms (Sandhyarani and Pradeep 2001), oriented in three dimension which produce multiple series of peaks as shown in Fig. 4. Intense periodic diffraction patterns with large d spacing provided evidence for the presence of those layers. Interlayer spacing, d was almost equal to twice the length of alkyl chains because each CuS layer is separated by two alkyl chains. Those periodic reflections have been indexed as $(0k_i0)$ (Espinet et al. 1999; Parikh et al. 1999). Cu_2S reflections match with the standard.

Conclusion

In summary, we have prepared a PET-protected copper cluster for the first time. From the MALDI MS data, a molecular ion peak at m/z 5,800 has been identified and it is assigned to $\sim Cu_{38}(PET)_{25}$. However, the cluster decomposes in about 2 h at room temperature forming a mixture of copper thiolates and cuprous sulphide as characterised by PXRD. It is important to improve the atmospheric stability to find new applications for these systems.

Acknowledgments We thank the Department of Science and Technology, Government of India for financial support. Thanks are due to SAIF, IIT Madras for the PXRD data.

References

Ai Z, Zhang L, Lee S, Ho W (2009) Interfacial hydrothermal synthesis of Cu@Cu_2O core-shell microspheres with enhanced visible-light-driven photocatalytic activity. J Phys Chem C 113(49):20896. doi:10.1021/jp9083647

Bakshi MS, Possmayer F, Petersen NO (2007) Simultaneous synthesis of Au and Cu nanoparticles in pseudo-core-shell type arrangement facilitated by DMPG and 12-6-12 capping agents. Chem Mater 19(6):1257. doi:10.1021/cm062771t

Bootharaju MS, Pradeep T (2011) Investigation into the reactivity of unsupported and supported Ag_7 and Ag_8 clusters with toxic metal ions. Langmuir 27(13):8134. doi:10.1021/la200947c

Chaki NK, Negishi Y, Tsunoyama H, Shichibu Y, Tsukuda T (2008) Ubiquitous 8 and 29 kDa gold:alkanethiolate cluster compounds: mass-spectrometric determination of molecular formulas and structural implications. J Am Chem Soc 130(27):8608. doi:10.1021/ja8005379

Chakraborty I, Govindarajan A, Erusappan J, Ghosh A, Pradeep T, Yoon B, Whetten RL, Landman U (2012a) The superstable 25 kDa monolayer protected silver nanoparticle: measurements and interpretation as an icosahedral $Ag_{152}(SCH2CH2Ph)_{60}$ cluster. Nano Lett 12(11):5861–5866. doi:10.1021/nl303220x

Chakraborty I, Udayabhaskararao T, Pradeep T (2012b) High temperature nucleation and growth of glutathione protected $\sim Ag_{75}$ clusters. Chem Commun 48(54):6788

Dass A (2009) Mass spectrometric identification of $Au_{68}(SR)_{34}$ molecular gold nanoclusters with 34-electron shell closing. J Am Chem Soc 131(33):11666. doi:10.1021/ja904713f

Dhanalakshmi L, Udayabhaskararao T, Pradeep T (2012) Conversion of double layer charge-stabilized Ag@citrate colloids to thiol passivated luminescent quantum clusters. Chem Commun 48(6):859. doi:10.1039/c1cc15604g

Espinet P, Lequerica MC, Martin-Alvarez JM (1982) Synthesis, structural characterization and mesogenic behavior of copper(I) *n*-alkylthiolates. Chem Eur J 5(7):1982–1986. doi:10.1002/(sici)1521-3765(19990702)5:7

Ghijsen J, Tjeng LH, Van EJ, Eskes H, Westerink J, Sawatzky GA, Czyzyk MT (1988) Electronic structure of cuprous and cupric oxides. Phys Rev B 38(16-A):11322

Ghodselahi T, Vesaghi MA, Shafiekhani A, Baghizadeh A, Lameii M (2008) XPS study of the Cu@Cu_2O core-shell nanoparticles. Appl Surf Sci 255(5):2730. doi:10.1016/j.apsusc.2008.08.110

Goswami N, Giri A, Bootharaju MS, Xavier PL, Pradeep T, Pal SK (2011) Copper quantum clusters in protein matrix: potential sensor of Pb^{2+} ion. Anal Chem 83(24):9676. doi:10.1021/ac202610e

Guo J, Kumar S, Bolan M, Desireddy A, Bigioni TP, Griffith WP (2012) Mass spectrometric identification of silver nanoparticles: the case of $Ag_{32}(SG)_{19}$. Anal Chem 84(12):5304. doi:10.1021/ac300536j

Habeeb MMA, Pradeep T (2011) Au_{25}@SiO2: quantum clusters of gold embedded in silica. Small 7(2):204

Haruta M (2005) Catalysis: gold rush. Nature 437(7062):1098. doi:10.1038/4371098a

Jadzinsky PD, Calero G, Ackerson CJ, Bushnell DA, Kornberg RD (2007) Structure of a thiol monolayer-protected gold nanoparticle at 1.1 a resolution. Science 318(5849):430

Jia X, Li J, Han L, Ren J, Yang X, Wang E (2012) DNA-hosted copper nanoclusters for fluorescent identification of single nucleotide polymorphisms. ACS Nano 6(4):3311. doi:10.1021/nn3002455

Knoppe S, Dharmaratne AC, Schreiner E, Dass A, Burgi T (2010) Ligand exchange reactions on Au_{38} and Au_{40} clusters: a combined circular dichroism and mass spectrometry study. J Am Chem Soc 132(47):16783. doi:10.1021/ja104641x

Lu Y, Chen W (2012) Sub-nanometer sized metal clusters: from synthetic challenges to the unique property discoveries. Chem Soc Rev 41(9):3594. doi:10.1039/c2cs15325d

Mathew A, Sajanlal PR, Pradeep T (2011) A fifteen atom silver cluster confined in bovine serum albumin. J Mater Chem 21(30):11205. doi:10.1039/c1jm11452b

Mathew A, Sajanlal PR, Pradeep T (2012) Selective visual detection of TNT at the sub-zeptomole level. Angew Chem Int Ed 51(38):9596–9600. doi:10.1002/anie.201203810

Muhammed MAH, Verma PK, Pal SK, Kumar RCA, Paul S, Omkumar RV, Pradeep T (2009) Bright, NIR-emitting Au_{23} from Au_{25}: characterization and applications including biolabeling. Chem Eur J 15(39):10110. doi:10.1002/chem.200901425

Nishida N, Miyashita A, Hashimoto N, Murayama H, Tanaka H (2011) Regenerative synthesis of copper nanoparticles by photoirradiation. Eur Phys J D 63(2):307. doi:10.1140/epjd/e2011-10515-8

Parikh AN, Gillmor SD, Beers JD, Beardmore KM, Cutts RW, Swanson BI (1999) Characterization of chain molecular assemblies in long-chain, layered silver thiolates: a joint infrared spectroscopy and X-ray diffraction study. J Phys Chem B 103(15):2850. doi:10.1021/jp983938b

Pei Y, Gao Y, Zeng XC (2008) Structural prediction of thiolate-protected Au_{38}: a face-fused bi-icosahedral Au core. J Am Chem Soc 130(25):7830. doi:10.1021/ja802975b

Prucek R, Kvitek L, Panacek A, Vancurova L, Soukupova J, Jancik D, Zboril R (2009) Polyacrylate-assisted synthesis of stable copper nanoparticles and copper(I) oxide nanocubes with high catalytic efficiency. J Mater Chem 19(44):8463. doi:10.1039/b913561h

Rao TUB, Pradeep T (2010) Luminescent Ag_7 and Ag_8 clusters by interfacial synthesis. Angew Chem Int Ed 49(23):3925. doi:10.1002/anie.200907120

Rao TUB, Nataraju B, Pradeep T (2010) Ag_9 quantum cluster through a solid-state route. J Am Chem Soc 132(46):16304. doi:10.1021/ja105495n

Retnakumari A, Setua S, Menon D, Ravindran P, Muhammed H, Pradeep T, Nair S, Koyakutty M (2010) Molecular-receptor-specific, non-toxic, near-infrared-emitting Au cluster-protein nanoconjugates for targeted cancer imaging. Nanotechnology 21(5):055103

Salorinne K, Chen X, Troff RW, Nissinen M, Haekkinen H (2012) One-pot synthesis and characterization of sub-nanometre-size benzotriazolate protected copper clusters. Nanoscale 4(14):4095. doi:10.1039/c2nr30444a

Sandhyarani N, Pradeep T (2001) An investigation of the structure and properties of layered copper thiolates. J Mater Chem 11(4):1294. doi:10.1039/b009837j

Saumya V, Rao TP (2012) Copper quantum cluster–polypyrrole composite film based zero current chronopotentiometric sensor for glutathione. Anal Methods 4(7):1976

Shibu ES, Muhammed MAH, Tsukuda T, Pradeep T (2008) Ligand exchange of $Au_{25}SG_{18}$ leading to functionalized gold clusters: spectroscopy, kinetics, and luminescence. J Phys Chem C 112(32):12168. doi:10.1021/jp800508d

Shichibu Y, Negishi Y, Tsukuda T, Teranishi T (2005) Large-scale synthesis of thiolated Au_{25} clusters via ligand exchange reactions of phosphine-stabilized Au_{11} clusters. J Am Chem Soc 127(39):13464. doi:10.1021/ja053915s

Stellwagen D, Weber A, Bovenkamp GL, Jin R, Bitter JH, Kumar CSSR (2012) Ligand control in thiol stabilized Au_{38} clusters. RSC Adv 2(6):2276. doi:10.1039/c2ra00747a

Udayabhaskararao T, Sun Y, Goswami N, Pal SK, Balasubramanian K, Pradeep T (2012) Ag_7Au_6: a 13-atom alloy quantum cluster. Angew Chem Int Ed 51(9):2155–2159. doi:10.1002/anie.201107696

Vilar-Vidal N, Blanco MC, Lo̓pez-Quintela MA, Rivas J, Serra C (2010) Electrochemical synthesis of very stable photoluminescent copper clusters. J Phys Chem C 114(38):15924. doi:10.1021/jp911380s

Wei Y, Chen S, Kowalczyk B, Huda S, Gray TP, Grzybowski BA (2010) Synthesis of stable, low-dispersity copper nanoparticles and nanorods and their antifungal and catalytic properties. J Phys Chem C 114(37):15612. doi:10.1021/jp1055683

Wei W, Lu Y, Chen W, Chen S (2011) One-pot synthesis, photoluminescence, and electrocatalytic properties of subnanometer-sized copper clusters. J Am Chem Soc 133(7):2060. doi:10.1021/ja109303z

Xavier PL, Chaudhari K, Baksi A, Pradeep T (2012) Protein-protected luminescent noble metal quantum clusters: an emerging trend in atomic cluster nanoscience. Nano Rev 3:14767. doi:10.3402/nano.v3i0.14767

Xie S, Tsunoyama H, Kurashige W, Negishi Y, Tsukuda T (2012) Enhancement in aerobic alcohol oxidation catalysis

of Au_{25} clusters by single Pd atom doping. ACS Catal 2(7):1519. doi:10.1021/cs300252g

Yuan X, Luo Z, Zhang Q, Zhang X, Zheng Y, Lee JY, Xie J (2011) Synthesis of highly fluorescent metal (Ag, Au, Pt, and Cu) nanoclusters by electrostatically induced reversible phase transfer. ACS Nano 5(11):8800–8808. doi:10.1021/nn202860s

Zhu M, Lanni E, Garg N, Bier ME, Jin R (2008) Kinetically controlled, high-yield synthesis of Au_{25} clusters. J Am Chem Soc 130(4):1138. doi:10.1021/ja0782448